Physics – Uspekhi **40** (10) 1069 – 1079 (1997)

CONFERENCES AND SYMPOSIA PACS number: 01.10.Fv

Scientific session of the Division of General Physics and Astronomy of the Russian Academy of Sciences (14 May 1997)

A scientific session of the Division of General Physics and Astronomy of the Russian Academy of Sciences was held on 14 May 1997 at the P L Kapitza Institute for Physical Problems, RAS. The following reports were presented at the session:

(1) **Mineev V P, Vavilov M G** (Landau Institute of Theoretical Physics, RAS, Chernogolovka, Moscow Region) "De Haas – van Alphen effect in superconductors";

(2) **Volkov V A, Takhtamirov É E** (Institute of Radioengineering and Electronics, RAS, Moscow) "Dynamics of an electron with space-dependent mass and the effective-mass method for semiconductor heterostructures";

(3) **Sukhorukov A P** (M V Lomonosov Moscow State University, Moscow) "New avenue of investigation in the physics of solitons: parametrically-coupled solitons in a quadratically-nonlinear medium";

(4) **Bogatov A P** (P N Lebedev Physics Institute, RAS, Moscow) "Optics of semiconductor lasers";

(5) **Korovin S D** (Institute of High-Power Electronics, Tomsk) "Generation of high-power microwave radiation on the base of high-current nanosecond electron beams";

(6) **Ardelyan N V, Bisnovatyĭ-Kogan G S, Moiseenko S G** (M V Lomonosov Moscow State University, Moscow; Institute of Space Research, Moscow) "Explosion mechanisms of supernovae: the magnetorotational model";

(7) **Slysh V I** (Astrocosmic Centre of the P N Lebedev Physics Institute, RAS, Moscow) "Stars, planets, and cosmic masers".

Summaries of four (1, 2, 6, 7) of the reports are given below.

PACS numbers: **05.50.+q**, **75.90.+w**

De Haas – van Alphen effect in superconductors

V P Mineev, M G Vavilov

The quantum oscillations of magnetization or, alternatively, the de Haas – van Alphen (dHvA) effect, is a well-studied phenomenon in the physics of normal metals. According to the universally accepted Lifshitz – Kosevich theory [1], each extreme section of the Fermi surface contributes to the oscillating part of the magnetization to yield

$$M_{\rm osc} \sim \sqrt{H}\,\frac{2\pi^2 T/\omega_{\rm c}}{\sinh(2\pi^2 T/\omega_{\rm c})}\exp\left(-\frac{\pi}{\omega_{\rm c}\tau}\right)\sin\left(\frac{2\pi F}{H}+\Phi\right). \quad (1)$$

Here $\omega_{\rm c} = eH/m^*c$ is the cyclotron frequency, $F = cS/2\pi e$, S is the area of the extreme section of the Fermi surface, and τ is the electron-vacancy scattering time. The Planck constant $\hbar$ is presumed hereafter to be equal to 1. The quantity $1/2\pi\tau$ is commonly referred as the Dingle temperature. Both the temperature and impurity-dependent factors in formula (1) fall rapidly with decreasing magnetic field, so that in normal metals dHvA oscillations are observable in sufficiently high fields. In the case of superconductors, the magnetic fields in which the dHvA effect is accessible to observation usually far exceed the critical field of the superconducting-normal phase transition. Therefore, the marked oscillations of magnetization would be expected to appear only in the region of very low temperatures

$$T < \frac{eH_{\rm c2}}{2\pi^2 m^* c} \sim \frac{T_{\rm c}^2}{\mu}\,. \quad (2)$$

Here $T_{\rm c}$ is the transition temperature in a zero magnetic field, and μ is the Fermi energy. On the other hand, because of electron-vacancy scattering [2], dHvA oscillations come into prominence only in sufficiently pure metals, i.e. when the condition $\omega_{\rm c}\tau \gg 1$ or, equivalently, $l_{\rm imp} \gg R_{\rm c}$, is fulfilled. Here $l_{\rm imp} = v_{\rm f}\tau$ is the mean free path, and $R_{\rm c} = k_{\rm f}\lambda^2$ is the cyclotron radius with $k_{\rm f}$ being the Fermi wave vector and $\lambda = \sqrt{c/eH}$ the magnetic length. In magnetic fields of the order of $H_{\rm c2}$, the quantity λ coincides with the coherence length $\xi(T)$. Therefore, the requirements on the sample purity which would be sufficient to observe dHvA oscillations in fields of the order of $H_{\rm c2}$, viz.

$$l_{\rm imp} \gg k_{\rm f}\xi^2\,, \quad (3)$$

is much more stringent than the conventional condition on semiconductor purity $l_{\rm imp} \gg \xi_0$.

Thus, observations of the dHvA effect in the regions of fields and temperatures typical of type II superconductors are possible only in the case of ultra-pure superconductors with a large magnitude of the upper critical field, which are rather rare. Among these are compounds with the A-15 structure (V_3Si, Nb_3Sn) [3, 4], boron carbides ($YNiB_2C$) [5] as well as some organic and layered superconductors (see the reviews [6, 7]). For example, in V_3Si [3] where $H_{\rm c2} = 18.5$ T, $T_{\rm c} = 17$ K, $\xi_0 = 6.3$ nm and $l_{\rm imp} > R_{\rm c} = 130$ nm, dHvA oscillations in fields of the order of $H_{\rm c2}$ are accessible to observation at temperatures of the order of 1 K.

Uspekhi Fizicheskikh Nauk **167** (10) 1121 – 1131 (1997)
Translated by V M Matveev, K A Postnov; edited by A Radzig

The dHvA effect in these substances remains when going to the mixed state ($H < H_{c2}$). In this state, the oscillation frequency does not change, whereas the amplitude falls with decreasing field more rapidly than in the normal state.

The suppression of the magnetization-oscillation amplitude in type II superconductors was calculated in the theoretical works [8] and [9]. It was shown that quasi-particle scattering by the nonuniform spatial distribution of the order parameter $\Delta(\mathbf{R})$ in the mixed state results in an additional broadening of the Landau levels:

$$\frac{1}{\tau_s} \sim \sqrt{\mu\omega_c}\,\frac{H_{c2}-H}{H_{c2}}\,. \tag{4}$$

As a result, the amplitude of the dHvA effect attains, apart from the Dingle factor, another temperature-independent multiplier $\exp(-\pi/\omega_c\tau_s)$ and decreases rather rapidly away from the phase transition line H_{c2}.

The derivation of expression (4) is inadequate from the theoretical standpoint. The matter is that the electron spectrum and the level broadening were obtained by Maki [8] through formally replacing the quasi-classical spectrum found by Brandt et al. [10] with the corresponding quantum expression. The quasi-classical description in terms of the continuous variables $\xi = k^2/2m - \mu$ and polar angle θ is quite adequate when the distance between the Landau levels is small in comparison with temperature T or level width $\Gamma = 1/2\tau$. When studying the dHvA effect, we are dealing with the opposite situation $\omega_c > 2\pi^2 T$ and $\omega_c > \pi\Gamma$, so that the quasi-classical approach is inapplicable for calculation of the spectrum.

Nevertheless, the quantum approach developed by Stephen [9] has strengthened the results by Maki [8]. However, when calculating the quasi-particle-energy eigenvalue in the limit of low temperatures $T < \omega_c$ [9], the summation over the principle quantum number was replaced with the integration that is admissible only in the case when the width of the levels exceeds the distance between them. That was the reason why the results by Stephen [9] and Maki [8] turned out the same.

Some other descriptions of the dHvA effect in superconductors were also proposed [11–13]. Different approaches were put forward, but in one way or another the BCS-type spectrum was used, namely

$$E = \sqrt{E_n^2(k_z) + \Delta^2}\,, \tag{5}$$

where

$$E_n(k_z) = \omega_c\left(n + \frac{1}{2}\right) + \frac{k_z^2}{2m} - \mu\,. \tag{6}$$

Stephen [9] showed that spectrum (5) is realized only in sufficiently weak fields $\sqrt{\mu\omega_c} \ll T$, therefore, in view of Eqn (2), magnetization oscillations in this region are not observable.

Formally, spectrum (5) is also derived in the ultra-quantum limit $\omega_c \sim \mu$ [14]. However, it is known that in the ultra-quantum limit the mean-field approximation in the theory of superconductivity is inapplicable (see Ref. [15]) and, thus, the mathematical model used in Ref. [14] does not provide an adequate description of superconductivity in strong magnetic fields.

We developed a self-consistent quantum theory of the dHvA effect in the mixed state [16]. It was shown that at a finite concentration of impurities, despite the requirement of high purity $\omega_c > \pi\Gamma$ that is necessary to observe the dHvA effect, in the mixed state near the upper critical field H_{c2} a region of gapless superconductivity exists, in which the density of states on the Fermi surface remains finite, i.e.

$$N(E=0) = N_0\left(1 - \frac{2\sqrt{\pi^3 n_f}}{L\ln n_f}\,\frac{H_{c2}-H}{H_{c2}}\right). \tag{7}$$

Here N_0 is the density of states in the normal metal, $n_f = \mu/\omega_c$, and L is a numerical constant, $L \approx 2$.

According to Eqn (7), in the vicinity of the metal–superconductor phase transition there is a region of gapless superconductivity in the field range

$$\frac{H_{c2}-H}{H_{c2}} < \frac{\ln n_f}{\pi^{3/2}\sqrt{n_f}}\,. \tag{8}$$

For the most superconductors the number n_f is rather large. Because of this, the gapless superconductivity is realized in a very narrow range of magnetic fields. Nevertheless, n_f does not exceed 50 for superconductors in which dHvA oscillations were observed [3, 4]. In accordance with Eqn (8), the density of states at the Fermi level remains finite at $H_{c2} - H \approx 0.1H_{c2}$.

The oscillating part of the density of states at the Fermi level and hence the oscillating part of the magnetization M_s^{osc} is also suppressed in the mixed state relative to its value M_n^{osc} in the normal state:

$$\frac{M_s^{osc}}{M_n^{osc}} = 1 - \frac{2\sqrt{\pi n_f}}{L\ln n_f}\,\frac{H_{c2}-H}{H_{c2}}\,. \tag{9}$$

Expressions (7) and (9) were obtained in the linear approximation with respect to the square of the order parameter $\Delta^2 \sim (H_{c2}-H)/H_{c2}$ with the proviso that $T < \Gamma \ll \omega_c$. Going beyond the scope of the linear approximation presents serious mathematical problems resulting from the nondiagonality of the energy-eigenvalue matrix, which necessarily occurs because of the irregular spatial distribution of the order parameter.

References

1. Lifshitz I M, Kosevich A M *Zh. Eksp. Teor. Fiz.* **29** 730 (1955) [*Sov. Phys. JETP* **2** 636 (1956)]
2. Bychkov Yu A *Zh. Eksp. Teor. Fiz.* **39** 1401 (1961) [*Sov. Phys. JETP* **12** 977 (1961)]
3. Corcoran R et al. *Phys. Rev. Lett.* **72** 701 (1994)
4. Harrison N et al. *Phys. Rev. B* **50** 4208 (1994)
5. Goll G et al. *Phys. Rev. B* **53** 8871 (1996)
6. Corcoran R et al. *Physica B* **206–207** 534 (1995)
7. Springford M, Wasserman A *J. Low Temp. Phys.* **105** 273 (1996)
8. Maki K *Phys. Rev. B* **44** 2861 (1991)
9. Stephen M J *Phys. Rev. B* **45** 5481 (1992)
10. Brandt U, Pesch W, Tewordt L *Z. Phys.* **201** 209 (1967)
11. Dukan S, Tesanovic Z *Phys. Rev. Lett.* **74** 2311 (1995)
12. Miller P, Györffy B L *J. Phys.: Condens. Matter* **7** 5579 (1995)
13. Miyake K *Physica B* **186–188** 115 (1993)
14. Rasolt M, Tesanovic Z *Rev. Mod. Phys.* **64** 709 (1992)
15. Yakovenko V M *Phys. Rev. B* **47** 8851 (1993)
16. Vavilov M G, Mineev V P *Zh. Eksp. Teor. Fiz.* (in press)

PACS numbers: 71.25.Cx, 73.20.Dx, 73.40.Kp

Dynamics of an electron with space-dependent mass and the effective-mass method for semiconductor heterostructures

V A Volkov, É E Takhtamirov

1. Introduction

For a quantum-mechanical description of the electron dynamics in crystals in smoothly-varied external fields, the effective-mass (EM) method, or approximation, is widely used. As applied to homogeneous semiconductors, this method was developed by Luttinger and Kohn [1, 2] 40 years ago. The mathematical basis for the Kohn – Luttinger approach is the envelope-function (EF) method. The case in point is functions which vary slowly over distances of the order of the lattice parameter a. With the advent and development of the physics of semiconductor heterostructures and their practical use in devices (suffice it to point to a multiplicity of uses of multilayer heterostructures with quantum wells), the question arose on the extension of the EM method to the case of space-dependent EM $m(\mathbf{r})$. Over the past 30 years many varied formulations of this question have been proposed. Among the relevant problems we note two obvious ones. The first is the lack of uniqueness of the kinetic-energy operator resulting from the noncommutativity of the momentum operator and the function $m(\mathbf{r})$. *A priori* this operator must be no more than an Hermitian one; this imposes a rather weak restriction on its possible form which may strongly affect the solutions of the EM equation [3]. The second problem lies in the fact that the effective potential near a heterojunction in many cases is not a smoothly-varying function over distances of the order of a. This casts some doubt upon the validity of using differential equations in the framework of the EM method.

We shall restrict our consideration to heterostructures consisting of related substances when the boundary band-energy jumps are small in comparison with the typical energy-gap widths; as a rule, this also implies a small difference between EM parameters. Let us discuss the first problem which arises even for heterojunctions (HJ) with a gradual change of the chemical composition over distances of the order of a. Choose the crystal-lattice potential of one of materials (mentally extended to all space) as a zeroth-approximation potential and consider the distinctions of the lattice potentials of other semiconductors from the basis one as perturbations. Following the Kohn – Luttinger approach and obtaining the multiband $\mathbf{k}\cdot\mathbf{p}$-system of equations (see, for example, Ref. [4]), an effort can be made to resolve the problem of the proper order of noncommutative operators in the kinetic-energy operator for 'single-band' equations (one equation being valid near the bottom of the conduction band or the system of equations near the top of the valence band).

Reducing the multiband system of equations to the single-band equation is accomplished through elimination of the small EFs from the multiband $\mathbf{k}\cdot\mathbf{p}$-system using a certain procedure. Here, it is pertinent to make a small digression and use a formal analogy between the relativistic Dirac equation and the multiband $\mathbf{k}\cdot\mathbf{p}$-system of equations on EF [5], which is most easily traced in the two-band approximation (conduction and valence bands). In the relativistic theory, there are two approaches to obtain equations for the 'shallow' states of electrons. The first approach consists in expressing the small positron component of the wave function via the electron wave function and substituting this component into the electron-component equation. In doing so, one can deal with either an exact equation which is not the eigenvalue equation ([6], Chapter XX, Section 28) or an approximate equation whose Hermitian behaviour should be tracked individually [7]. Another approach is the use of the Foldy – Wouthuysen-type transformation, i.e. the approximate unitary transformation of the Dirac equation ([6], Chapter XX, Section 33). In our case the first approach is realized without problems only in the two-band approximation (see, for example, Ref. [8]); when taking into consideration remote bands, some difficulties emerge [9,10]. This point is essential for describing hole states in III – V semiconductor structures since the finiteness of the EM of heavy holes is achieved beyond the framework of the two-band model. Therefore, we will follow the second approach, which uses a unitary transformation eliminating small EFs ([11], Section 15). Since we are considering heterostructures consisting of related materials, the canonical Kohn – Luttinger method with space-independent effective mass will play the role of the first approximation. Allowance for the spatial dependence of the EM will generate a need for consideration of corrections to the canonical theory. All corrections of the same order of smallness should be taken into account, allowing no excess of accuracy. Turn now to a relativistic analogy with a hypothetical Dirac equation involving an irregular gap $2c^2m(\mathbf{r})$, where c is the speed of light in a vacuum. The conventional single-band EM equation is analogous to the nonrelativistic Schrödinger equation. It is significant, however, that the EM in the two-band approximation is proportional to the local energy-gap width $E_g(\mathbf{r})$ and the relative variation of the EM comprises $\delta m/m \simeq \delta E_g/E_g$. By virtue of the fact that the correction to the kinetic energy describing the spatial dependence of the EM would be 'relativistic' in character ($\delta m/m \propto 1/c^2$), the required equations for HJ will be analogous to the Schrödinger equation which includes all relativistic corrections proportional to $1/c^2$, both the conventional corrections (the contribution of nonparabolicity which is proportional to $\mathbf{p}^4$, where $\mathbf{p}$ is the momentum operator, the contribution of the spin-orbit interaction and the Darwin term) and a new pseudo-relativistic correction describing $\delta m(\mathbf{r})$.

A voluminous, even if far from complete, bibliography on attempts to obtain the EM equations with space-dependent band parameters is contained in Ref. [10]. Some of these publications were discussed in Ref. [12] where the multiband $\mathbf{k}\cdot\mathbf{p}$-system of equations was reduced with the use of a unitary transformation to the approximate single-band equation describing the conduction-band states near the Γ-point in (001) heterostructures. In this paper, the main drawback of all the previous works was pointed out, namely, not taking into account all the terms of the same order of smallness. Here one cannot but mention that for homogeneous semiconductors the EM equation analogous to the Schrödinger equation with the first relativistic corrections was discussed still in Ref. [11] (Section 27).

The second problem which arises in the EF method is the lack of smoothness of real HJ when the transition-region width between two materials is of the order of a. In this case, firstly, the Leibler's multiband $\mathbf{k}\cdot\mathbf{p}$-system calls for refine-

ment [4] and, secondly, the problem of the inverse Fourier transformation in **k**-space confined by the first Brillouin zone is complicated [1]. These transformations lead to a set of cumbersome and inconvenient integro-differential equations. Their reduction to differential equations may be accomplished only with some sacrifice in the accuracy of the method. The resulting error must be also estimated. The estimation of this error either gives assurance in the absence of an excess of accuracy or casts some doubt on the validity of the EM approximation (notice that in the literature, including papers [13] and [10], such an estimate is missing).

Below, only one of approaches to the formulation of the EM approximation for heterostructures is discussed, namely, the derivation of an effective Hamiltonian which is defined in all coordinate space. In doing so, the smallness of $E_g(\mathbf{r})$ variations is used. There is also another approach being applied only to structures with mathematically sharp HJ. This is the introduction of boundary conditions (BC) for EF at the interface between two different semiconductors. In this case, a problem arises of the determination of the function space in which the effective Hamiltonian is defined [12]. (The exception is the HJ between two semiconductors with a very large difference in the energy-gap width or the semiconductor–insulator junction. In this limit, it is sufficient to derive the boundary conditions only for EFs describing the low-energy-gap semiconductor [14–16].) Once the single-band equations take into account the difference in EM parameters, they must generally include all the above-discussed pseudo-relativistic corrections, therefore, drawbacks become evident in the approaches used, for example, in Refs [17, 18] where the BC for EF were derived, the latter being the solutions of the canonical EM equation.

Thus, we can state the following stages of the construction of a correct EM approximation for heterostructures: (a) obtaining the correct multiband $\mathbf{k}\cdot\mathbf{p}$-system of equations on EF; (b) reducing this system to single-band equations through a unitary transformation in **k**-space; (c) conversion to the **r**-representation, transformation of the equation obtained to a differential form and estimation of the accuracy of such a transformation. Following this scheme, stage (a) is realized in Section 2. The equations include the contributions determined by the lack of smoothness of HJ over distances of the order of a, which are considered in the context of the approach used in Ref. [11] for a description of a short-range potential. The main limitation on the accuracy of the differential equations in the EF method for sharp HJ follows from the inverse-Fourier-transform procedure in the final **k**-space (Section 3). In Section 4.1, the applicability of single-band equations is discussed. And the effects related to the lack of smoothness of HJ are considered in Section 4.2 (conduction band) and 4.3 (valence band).

2. Multiband $\mathbf{k}\cdot\mathbf{p}$-system of equations

Consider a structure with one HJ formed from related lattice-parameter-matched semiconductors having a SZn-type (zinc blende) crystal structure. For simplicity, we shall restrict our consideration to the following model of the crystal potential for this structure:

$$U = U_1 + G\big[U_2 - U_1\big] \equiv U_1 + G\delta U\,,$$

where $U_1 \equiv U_1(\mathbf{r})$ and $U_2 \equiv U_2(\mathbf{r})$ are the periodical potentials (with the same period) of left and right materials, respectively, extended to all the structure, the z-axis is perpendicular to the HJ plane, and $G \equiv G(z)$ is the HJ form-factor [$G(z<-d)=0$, $G(z>d)=1$ with $2d$ being the transition-region width].

As the basis for the expansion of the total wave function $\Psi(\mathbf{r})$, we shall use the full set of the orthonormalized Kohn–Luttinger functions $u_{n0}\exp(\mathrm{i}\mathbf{k}\cdot\mathbf{r})$, where $u_{n0} \equiv u_{n0}(\mathbf{r})$ is the Bloch function for the edge ϵ_{n0} of the nth band of the left crystal in the $\mathbf{\Gamma}$-point:

$$\Psi(\mathbf{r}) = \sum_{n'} \int \mathrm{d}\mathbf{k}'\mathcal{F}_{n'}(\mathbf{k}')\exp(\mathrm{i}\mathbf{k}'\cdot\mathbf{r})u_{n'0}\,.$$

The summation is over all zones, whereas the integration is, except as otherwise noted, over the first Brillouin zone; $\mathcal{F}_n(\mathbf{k})$ presents the EF for the nth zone in the **k**-representation. Following the standard procedure [1], one can obtain the required $\mathbf{k}\cdot\mathbf{p}$-system of equations (the relativistic contributions will be considered below):

$$\left(\epsilon_{n0} + \frac{\hbar^2\mathbf{k}^2}{2m_0}\right)\mathcal{F}_n(\mathbf{k}) + \sum_{n'}\frac{\hbar\mathbf{p}_{nn'}\cdot\mathbf{k}}{m_0}\,\mathcal{F}_{n'}(\mathbf{k}) + \sum_{n'}\int \mathrm{d}\mathbf{k}'\mathcal{M}_{nn'}(\mathbf{k},\mathbf{k}')\mathcal{F}_{n'}(\mathbf{k}') = \epsilon\mathcal{F}_n(\mathbf{k})\,; \tag{1}$$

$$\mathcal{M}_{nn'}(\mathbf{k},\mathbf{k}') = \delta(\mathbf{k}_\parallel - \mathbf{k}'_\parallel) \times \left[\mathcal{G}(k_z - k'_z)\delta U_{nn'} + \sum_{j\neq 0} C_j^{nn'}\mathcal{G}(k_z - k'_z + K_j)\right]. \tag{2}$$

Here m_0 is the mass of a free electron, $\mathbf{p}_{nn'} = \langle n|\mathbf{p}|n'\rangle$, $\mathbf{k}_\parallel = (k_x, k_y, 0)$, $C_j^{nn'} = \langle n|\delta U\exp(\mathrm{i}K_j z)|n'\rangle$, $\delta U_{nn'} = C_0^{nn'}$, $K_j = (4\pi/a)j$, where $j = \pm1, \pm2, \ldots$ and $\mathcal{G}$ is the Fourier transform of function G; expression (2) is valid for a (001) heterostructure at $|k_x| + |k_y| < \pi/a$, where $Ox \parallel [100]$ and $Oy \parallel [010]$.

If $G(z)$ is a rather smooth function ($a \ll 2d$), we can neglect the second term in the square brackets of Eqn (2) and obtain the well-known set of equations on EF [4]. In the case of a sharp HJ, one can follow the method which was used in Ref. [11] for the description of a short-range potential:

$$\sum_{j\neq 0} C_j^{nn'}\mathcal{G}(k_z - k'_z + K_j) = \sum_{l=0,1,\ldots}(k_z - k'_z)^l D_{lnn'}\,. \tag{3}$$

The constants $D_{lnn'}$ are determined by the properties of the function $G' \equiv \mathrm{d}G/\mathrm{d}z$ in the following manner:

$$D_{0nn'} = \sum_{j\neq 0} C_j^{nn'}\frac{1}{2\pi\mathrm{i}K_j}\int_{-d}^{d} G'(z)\exp(-\mathrm{i}K_j z)\,\mathrm{d}z\,,$$

$$D_{1nn'} = \sum_{j\neq 0} C_j^{nn'}\frac{1}{2\pi\mathrm{i}K_j}\int_{-d}^{d} G'(z)\exp(-\mathrm{i}K_j z) \times\left(-\frac{1}{K_j} - \mathrm{i}z\right)\mathrm{d}z\,,\ldots$$

In principle, this approach is applied even to a mathematically sharp HJ. Thus, Eqns (1) in view of Eqns (2) and (3) determine the multiband $\mathbf{k}\cdot\mathbf{p}$-system of equations for a structure with one HJ. A generalization to the case of many HJs is elementary. In this case, it is convenient to define the coordinates of the heteroboundaries so that a whole number of $a/2$ is accommodated between them. This is always

possible for (001) heterostructures. Then the phase factor in each expansion of type (3) will be equal to 1.

Now consider the corrections associated with the sharpness of HJ. The terms which are proportional to $D_{0nn'}, D_{1nn'}, \ldots$ can give corrections of order of magnitude no more than $a\bar{k}_z, (a\bar{k}_z)^2, \ldots$, respectively. Here $\bar{k}_z$ is the inverse characteristic length for the EF variation. Our goal is to obtain single-band equations with space-dependent EM parameters that is accomplished when taking into account corrections of the order of $(\lambda\bar{k}_z)^2$ to the canonical approximation. Here $\lambda = (2mE_g)^{-1/2}$ (for GaAs $\lambda \approx 6$ A). Therefore in Eqn (3) it will suffice to consider the terms $l = 0$ and $l = 1$ only.

Let us next include relativistic effects. Consider the spin-orbit interaction using perturbation theory and assume that its characteristic value is of the order of a typical boundary band-energy jump. We shall restrict ourselves to just a spin-orbit interaction alone since other relativistic contributions will affect only the numerical values of the constants obtained. The following corrections will appear in the left-hand side of Eqns (1):

$$\sum_{n'} \frac{\hbar\langle n|[\nabla U_1 \times \mathbf{p}]|n'\rangle \cdot \boldsymbol{\sigma}}{4m_0^2c^2}\, \mathcal{F}_{n'}(\mathbf{k}) + \sum_{n'} \frac{\hbar\langle n|[\nabla \delta U \times \mathbf{p}]|n'\rangle \cdot \boldsymbol{\sigma}}{4m_0^2c^2} \int \mathcal{G}(k_z - k'_z)\mathcal{F}_{n'}(k'_z, \mathbf{k}_\parallel)\, \mathrm{d}k'_z + \sum_{n'} \int \left(\mathbf{S}_{0nn'} + (k_z - k'_z)\mathbf{S}_{1nn'}\right) \cdot \boldsymbol{\sigma}\mathcal{F}_{n'}(k'_z, \mathbf{k}_\parallel)\, \mathrm{d}k'_z\,.$$

Here $\boldsymbol{\sigma}$ presents the spin 1/2 matrices and the vectors $\mathbf{S}_{0nn'}$ and $\mathbf{S}_{1nn'}$ are defined in the following manner:

$$\mathbf{S}_{0nn'} = \int_{-d}^{d} G'(z)\exp(-\mathrm{i}K_j z)\,\mathrm{d}z \times \sum_{j\neq 0} \frac{\hbar\langle n|[\nabla(\exp(\mathrm{i}K_j z)\delta U) \times \mathbf{p}]|n'\rangle}{8\pi\mathrm{i}K_j m_0^2c^2}\,;$$

$$\mathbf{S}_{1nn'} = -\sum_{j\neq 0} \frac{\hbar\langle n|[\nabla(\exp(\mathrm{i}K_j z)\delta U) \times \mathbf{p}]|n'\rangle}{8\pi\mathrm{i}K_j m_0^2c^2} \times \int_{-d}^{d} G'(z)\exp(-\mathrm{i}K_j z)z\,\mathrm{d}z - \sum_{j\neq 0} \frac{\hbar\langle n|\exp(\mathrm{i}K_j z)[\nabla \delta U \times \mathbf{p}]|n'\rangle}{8\mathrm{i}\pi K_j^2 m_0^2c^2} \times \int_{-d}^{d} G'(z)\exp(-\mathrm{i}K_j z)\,\mathrm{d}z\,.$$

Here $\mathbf{n}$ is a unit vector along the z-axis, $\mathbf{n}G'(z) \equiv \nabla G(z)$. We do not consider the contributions, linear in $\mathbf{k}$, of the spin-orbit interaction. They either give corrections of the order of $(\lambda\bar{k}_z)^3$ (similar to the contribution responsible for the removal of spin degeneracy in the conduction band of a bulk semiconductor) which are neglected or renormalize the values of some parameters.

3. Problem of the inverse Fourier transformation in quasi-momentum space

Let us discuss one more problem arising in the EF method and relating to the consideration of reciprocal space confined by the first Brillouin zone (BZ). Consider the following equation on EF $f(k_z)$ in the $\mathbf{k}$-representation:

$$\int H(k_z - k'_z)f(k'_z)\,\mathrm{d}k'_z = \epsilon f(k_z)\,, \tag{4}$$

where k_z and k'_z are belong to BZ. In the $\mathbf{r}$-representation, Eqn (4) transforms to an integro-differential equation. The problem lies in the accuracy which can be achieved when obtaining the relevant differential equation in $\mathbf{r}$-space. Consider an equation similar to Eqn (4) but with k_z and k'_z belonging to all reciprocal space:

$$\int_{-\infty}^{+\infty} H(k_z - k'_z)g(k'_z)\,\mathrm{d}k'_z = \epsilon g(k_z)\,. \tag{5}$$

Eqn (5), in contrast with Eqn (4), reduces to a differential equation in the $\mathbf{r}$-representation. In order for equations (4) and (5) to be approximately equivalent, it is necessary that the function $g(k_z)$ should be small for $k_z \notin$ BZ. In the case of smooth perturbations, such a smallness is provided by an exponentially diminishing EF in $\mathbf{k}$-space. In the opposite case of sharp perturbations, EF will diminish in a power-series manner.

For an EF with one discontinuity $g(k_z) \propto (\delta\bar{g}/\bar{g})(k_z)^{-1}$ at large k_z when the exponential contribution associated with the effects of the smooth field is damped out [here $(\delta\bar{g}/\bar{g})$ is a characteristic relative function jump at the point of discontinuity in the $\mathbf{r}$-representation]. Providing the standard EM equations [1, 2] are postulated, the second derivative of the EF will be discontinuous with the relative value of the jump close to unity and the error resulting from the use of differential equations will be of order $(\bar{k}_z/K)^3$, where $K = 2\pi/a$.

For a quantum well of width L, one can consider two cases: $\bar{k}_z L \gtrsim 1$ and $\bar{k}_z L \ll 1$. In the first case, the error is of the same order as for a separate HJ, while in the second case it is of the order of $(\bar{k}_z L)^{-1}(\bar{k}_z/K)^3$. In the latter case we arrive at an approximation where the potential of a quantum well may be replaced by the delta-function with an error of the order of $(\bar{k}_z/K)^2$. We shall use these results in Section 4.

4. Single-band equations

4.1 Applicability of the single-band equations

In $\mathbf{k}$-space near the Γ-point, there exists a region Λ_1 in which one can use a perturbation theory series, converging when $k_z < 1/(2\lambda)$, for describing the interaction of the states of separated (closely-spaced) bands with the states of other bands (this follows from the two-band approximation). There also exists a region Λ_2 where the interaction with remote bands is not described by this series. In our case of a sharp HJ, the EFs in the $\mathbf{k}$-representation diminish in a power-series manner, therefore we must correctly describe the region Λ_2 as well. However, it can be shown that if the ratio of the characteristic values of the band-energy jump to the energy gap between the states of interest in the region Λ_1 and states in the region Λ_2 is a small parameter $r \ll 1$, then the error of ignoring the region Λ_2 will be of the order of $r(\lambda\bar{k}_z)^2$ or less.

Below we shall obtain the EM equation for the conduction band passing over the details of a unitary transformation in $\mathbf{k}$-representation and going over immediately to the $\mathbf{r}$-representation. Formally, the final equation will be a

differential equation of the fourth order and the EF obeying this equation will have a discontinuous second derivative with a characteristic jump, being of the order of the second derivative itself (just this will determine the error when going over to the differential equation). And this means that for a wide quantum well the accuracy of the EM equation obtained will be of the order of $(\bar{k}_z\lambda)^3$. In the case of a narrow quantum well ($L < \lambda$), the EM equation must include only the first corrections associated with the effects of the sharpness of the HJ, while a consideration of other corrections, including those responsible for the spatial dependence of the EM parameters, would result in an excess of accuracy.

4.2 Conduction band

For a smooth HJ, the single-band equation on EF for the c-band was obtained in Ref. [12]. In the **r**-representation it takes the form

$$\epsilon_{c0}F_c(\mathbf{r}) + \frac{1}{2}\,m^{\alpha}(z)\mathbf{p}m^{\beta}(z)\mathbf{p}m^{\alpha}(z)F_c(\mathbf{r}) + \mathbf{\Gamma}(z)\Delta U_c F_c(\mathbf{r}) + \alpha_0\mathbf{p}^4F_c(\mathbf{r}) + \beta_0(\mathbf{p}_{\parallel}^2p_z^2 + p_x^2p_y^2)F_c(\mathbf{r}) + \eta[\mathbf{p}\times\mathbf{n}]\cdot\boldsymbol{\sigma}\mathbf{\Gamma}'(z)F_c(\mathbf{r}) = \epsilon F_c(\mathbf{r})\,. \tag{6}$$

The boundary conduction-band jump ΔU_c, the modified form-factor $\mathbf{\Gamma}(z)$ and EM $m(z)$ are determined by the following expressions

$$\mathbf{\Gamma}(z)\Delta U_c = G(z)\delta U_{cc} + {\sum_n}' \frac{|\delta U_{cn}|^2}{\epsilon_{c0}-\epsilon_{n0}}\,G^2(z)\,,$$

$$m(z) = m_1\left[1 + m_1(\mu_2-\mu_1)\mathbf{\Gamma}(z)\right]^{-1},$$

$$\alpha = \frac{\mu_1}{2(\mu_2-\mu_1)}\,, \qquad 2\alpha+\beta=-1\,.$$

In Eqn (6), α_0 and β_0 are the nonparabolicity parameters of the volume spectrum and

$$\mu_1 = {\sum_n}' \frac{2\left|\langle c|p_x|n\rangle\right|^2\delta U_{cc}}{m_0^2(\epsilon_{c0}-\epsilon_{n0})^2} - {\sum_{n,l}}' \frac{4\langle c|p_x|n\rangle\langle n|p_x|l\rangle\delta U_{lc}}{m_0^2(\epsilon_{c0}-\epsilon_{n0})(\epsilon_{c0}-\epsilon_{l0})}\,,$$

$$\mu_2 = {\sum_{n,l}}' \frac{2\langle c|p_x|n\rangle\delta U_{nl}\langle l|p_x|c\rangle}{m_0^2(\epsilon_{c0}-\epsilon_{n0})(\epsilon_{c0}-\epsilon_{l0})}\,,$$

$$\eta = {\sum_{n,l}}' \frac{\hbar\langle c|p_z|n\rangle\langle n|[\nabla\delta U\times\mathbf{p}]_x|l\rangle\langle l|p_y|c\rangle}{4im_0^4c^2(\epsilon_{c0}-\epsilon_{n0})(\epsilon_{c0}-\epsilon_{l0})}\,.$$

The modified EF $F_c(\mathbf{r})$ is related to the total wave function $\Psi(\mathbf{r})$ through a cumbersome expression (see Ref. [12]).

To include the corrections associated with the lack of smoothness of HJ in Eqn (6), it should be taken into account that the contributions determined by the terms $D_{0nn'}$, $D_{1nn'}$, $\mathbf{S}_{0nn'}$ and $\mathbf{S}_{1nn'}$ must be considered in the first order of the perturbation theory, while the contributions from $D_{0nn'}$ and $\mathbf{S}_{0nn'}$ — in the second order as well (together with the terms $\hbar\mathbf{k}\cdot\mathbf{p}_{nn'}/m_0$). As a result, there will be an additional term $\hat{H}_{abr}$ in the Hamiltonian of Eqn (6):

$$\hat{H}_{abr} = D_{0cc}\delta(z) + \rho\delta'(z) + \tilde{\eta}[\mathbf{p}\times\mathbf{n}]\cdot\boldsymbol{\sigma}\,\delta(z)\,. \tag{7}$$

Let us represent function $G'(z)$ as a sum of the symmetric $\left[G_s'(z)\right]$ and antisymmetric $\left[G_a'(z)\right]$ parts. Then one obtains

$$D_{0cc} = -{\sum_{j\neq0}}\frac{\langle c|\delta U\cos(K_jz)|c\rangle}{2\pi K_j}\int_{-d}^{d}G_a'(z)\sin(K_jz)\,\mathrm{d}z\,,$$

$$\rho = {\sum_{j\neq0,\,n}}'\frac{\hbar\langle c|p_z|n\rangle\langle n|\delta U\sin(K_jz)|c\rangle}{2\pi(-i)K_jm_0(\epsilon_{c0}-\epsilon_{n0})}\int_{-d}^{d}G_s'(z)\cos(K_jz)\,\mathrm{d}z + {\sum_{j\neq0}}\frac{\langle c|\delta U\cos(K_jz)|c\rangle}{2\pi K_j} \times\int_{-d}^{d}G_s'(z)\left(\frac{\cos(K_jz)}{K_j}+z\sin(K_jz)\right)\mathrm{d}z\,,$$

$$\tilde{\eta} = {\sum_{j\neq0,\,n}}'\frac{\hbar\langle c|\left[\nabla(\sin(K_jz)\delta U)\times\mathbf{p}\right]_x|n\rangle\langle n|p_y|c\rangle}{4\pi K_jm_0^3c^2(\epsilon_{c0}-\epsilon_{n0})} \times\int_{-d}^{d}G_s'(z)\cos(K_jz)\,\mathrm{d}z\,.$$

Transform Eqn (6), taking into account Eqn (7), to a more compact form, valid for a sharp HJ ($2d\bar{k}_z \ll 1$). With an accuracy to terms of the order of $\max\left\{d\bar{k}_z(\lambda\bar{k}_z)^2, (d\bar{k}_z)^3\right\}$ (see Ref. [12]), one can obtain the final EM equation for a sharp HJ:

$$\epsilon_{c0}F_c(\mathbf{r}) + \frac{1}{2}\,m^{\tilde{\alpha}}(z)\mathbf{p}m^{\tilde{\beta}}(z)\mathbf{p}m^{\tilde{\alpha}}(z)F_c(\mathbf{r}) + \Theta(z)\Delta U_cF_c(\mathbf{r}) + \alpha_0\mathbf{p}^4F_c(\mathbf{r}) + \beta_0(\mathbf{p}_{\parallel}^2p_z^2 + p_x^2p_y^2)F_c(\mathbf{r}) + d_1[\mathbf{p}\times\mathbf{n}]\cdot\boldsymbol{\sigma}\,\delta(z)F_c(\mathbf{r}) + d_2\delta(z)F_c(\mathbf{r}) = \epsilon F_c(\mathbf{r})\,. \tag{8}$$

Here quantities $\tilde{\alpha}$, $\tilde{\beta}$, d_1 and d_2 take into consideration the finite width of the HJ, $2\tilde{\alpha}+\tilde{\beta}=-1$, $d_1=\eta+\tilde{\eta}$, and

$$d_2 = \Delta U_c\left(\int_{-d}^{d}\Gamma(z)dz - d\right) + D_{0cc}\,,$$

$\Theta(z)$ is the Heaviside step function, and lastly

$$\tilde{\alpha} = \frac{4\rho+\mu_1+2\Delta U_c\left[d^2-\int_{-d}^{d}2\mathbf{\Gamma}(z)z\,\mathrm{d}z\right]}{2(\mu_2-\mu_1-4\rho)}\,.$$

Let us analyze the Hamiltonian of Eqn (8). The first and third terms present the kinetic energy of an electron in the c-band. The second term is the space-dependent operator of the kinetic energy, quadratic in momentum (a general form of this operator was proposed in Ref. [19]). Notice that the parameter $\tilde{\alpha}$ is not a universal constant and depends both on the materials of the HJ and the form of the HJ transition region. The fourth and fifth terms in the Hamiltonian of Eqn (8) describe the corrections for the small nonparabolicity and are determined only by volume parameters. The sixth term describes the surface spin-orbit interaction (see, for example, Ref. [20]) whose intensity (d_1) depends not only on the materials of HJ, but also on the form of the transition region. The possibility of the existence of a contribution described by the seventh term was discussed in Ref. [21]; it is seen that this contribution vanishes for a mathematically sharp HJ.

In the case of a symmetric quantum well with two equivalent HJs (with coordinates $z=0$ and $z=L$), the

Hamiltonian for the c-band takes the form

$$\hat{H}^{el} = \epsilon_c(z) + \frac{1}{2}\, m^{\tilde{\alpha}}(z)\mathbf{p}m^{\tilde{\beta}}(z)\mathbf{p}m^{\tilde{\alpha}}(z) + \alpha_0\mathbf{p}^4F_c(\mathbf{r}) + \beta_0(\mathbf{p}_\parallel^2 p_z^2 + p_x^2\mathrm{p}_y^2)F_c(\mathbf{r}) + d_1[\mathbf{p}\times\mathbf{n}]\cdot\boldsymbol{\sigma}\{\delta(z) - \delta(z-L)\} + d_2\{\delta(z) + \delta(z-L)\},$$

where $\epsilon_c(z)$ describes the profile of the conduction-band edge.

4.3 Valence band

Let us briefly discuss the problem of the derivation of the EF equation for a valence band. There are two forms of this equation which frequently occur in the literature: the 'symmetrized' form (see, for example, Ref. [22]) and the equation obtained in Ref. [23]. Now, on derivation of the equation for a conduction band, we can point to the modifications which should be made in the EM method for the valence band to account for the spatial dependence of the EM parameters. Firstly, such an equation must include terms of the fourth order in the momentum operator (corrections for nonparabolicity) resulting from the interaction of the valence-band states with the states of other bands. Secondly, the characteristic parameters of band discontinuity and the spin-orbit interaction are, as a rule, of the same order, therefore the EM-equation Hamiltonian must have a 6×6 rather than 4×4 dimension, i.e. the interaction of heavy-hole, light-hole and spin-split bands must be considered 'exactly'. Thus, since the Luttinger's parameters are distinct from the EM parameters used in the conventional 6×6 equation (see Ref. [2]), three constants will be inadequate to specify the EM parameters for the valence band. The two above-mentioned versions of the EM equation for the valence band do not meet these requirements and can result in an excess of accuracy.

The derivation of an equation analogous to that obtained for the conduction band would constitute a rather cumbersome problem. Here we shall consider only an effect which is weak for bulk materials in smoothly-varied fields, namely, the mixing of heavy (hh) and light (lh) holes at the centre of the $2D$ Brillouin zone in (001) III–V heterostructures [24]. It can be demonstrated that the lack of smoothness of the HJ brings new operators into existence, which are responsible for this mixing in the Hamiltonian for valence-band states. Consider in the first order approximation only that the terms which are proportional to $D_{0\xi\xi'}$, where $\xi,\ \xi' = X, Y, Z$ are the Bloch functions at the top of the valence band, which transform in accordance with the representation $\boldsymbol{\Gamma}_{15}$. The nonvanishing off-diagonal matrix elements have the form

$$D_{0XY} = D_{0YX} = \sum_{j\neq 0} \frac{\langle X|U\sin(K_j z)|Y\rangle}{2\pi K_j} \int_{-d}^{d} G_s'(z)\cos(K_j z)\,\mathrm{d}z\,.$$

We write out the elements of the matrix Hamiltonian for the valence band, describing the lh–hh mixing:

$$\hat{H}^{\mathrm{hole}}_{h1,\,l2} = \hat{H}^{\mathrm{hole}}_{h2,\,l1} = \mathrm{i}\,\frac{D_{0XY}}{\sqrt{3}}\,\delta(z)\,,$$

where the indices $h1$, $h2$, $l1$ and $l2$ number the states of heavy and light holes (allowing for spin). An estimate of the constant in front of the δ-function was made in Ref. [24] by taking into account experimental data for heterostructures GaAs/AlAs: (100–300) meV A. It is seen, however, that this quantity depends on the structure of the interfaces, and the intensity of the mixing of heavy and light holes at the centre of the $2D$ Brillouin zone is greater for sharp HJs than for HJs with a smoothly-varied chemical composition. For a symmetric quantum well, one can obtain

$$\hat{H}^{\mathrm{hole}}_{h1,\,l2} = \hat{H}^{\mathrm{hole}}_{h2,\,l1} = \mathrm{i}\,\frac{D_{0XY}}{\sqrt{3}}\,\{\delta(z) - \delta(z-L)\}\,.$$

5. Conclusions

The envelope-function method developed by Kohn and Luttinger for the description of the electron structure of bulk semiconductors was generalized to the case of heterostructures formed by unstressed layers of related semiconductors with a SZn-type structure. For electron states near the $\boldsymbol{\Gamma}$-point in (001) heterostructures, the effective-mass equation which takes into account the spatial dependence of the effective mass and the possible sharpness of heterojunctions, was derived. The problem of derivation of an effective Hamiltonian for hole states in such structures was briefly outlined. It was shown that the lack of smoothness of heterojunctions results in mixing the states of heavy and light holes even at the centre of the Brillouin zone. The accuracy of the approach was also discussed.

The work was supported by the Russian Foundation for Basic Research (project 96-02-18811) and the Federal Programme "Physics of Solid-State Nanostructures" (project 1-094/4).

References

1. Luttinger J M, Kohn W *Phys. Rev.* **97** 869 (1955)
2. Luttinger J M *Phys. Rev.* **102** 1030 (1956)
3. Brezini A, Sebbani M, Marouf S *Phys. Status Solidi B* **189** 389 (1995)
4. Leibler L *Phys. Rev. B* **12** 4443 (1975)
5. Keldysh L V *Zh. Eksp. Teor. Fiz.* **45** 364 (1963) [*Sov. Phys. JETP* **18** 253 (1964)]
6. Messiah A *Quantum Mechanics* Vol. 2 (New York: Elsevier, 1976) [Translated into Russian (Moscow: Nauka, 1979)]
7. Berestetskiĭ V B, Lifshitz E M, Pitaevskiĭ L P *Kvantovaya Élektrodinamika* (Quantum Electrodynamics) par. 33 (Moscow: Nauka, 1972)
8. Suris R A *Fiz. Tekh. Poluprovodn.* **20** 2008 (1986) [*Sov. Phys. Semicond.* **20** 1258 (1986)]
9. Burt M G *Phys. Rev. B* **50** 7518 (1994)
10. Foreman B A *Phys. Rev. B* **54** 1909 (1996)
11. Bir G L, Pikus G E *Symmetry and Strain-Induced Effects in Semiconductors, Israel Program for Scientific Translations* (New York: Wiley, 1975) [Translated from Russian (Moscow: Nauka, 1972)]
12. Takhtamirov E E, Volkov V A *Semicond. Sci. Technol.* **12** 77 (1997)
13. Foreman B A *Phys. Rev. B* **52** 12241 (1995)
14. Volkov V A, Pinsker T N *Zh. Eksp. Teor. Fiz.* **70** 2268 (1976) [*Sov. Phys. JETP* **43** 1183 (1976)]
15. Volkov V A, Pinsker T N *Zh. Eksp. Teor. Fiz.* **72** 1087 (1977) [*Sov. Phys. JETP* **45** 568 (1977)]
16. Volkov V A, Pinsker T N *Fiz. Tverd. Tela* (Leningrad) **23** 1756 (1981) [*Sov. Phys. Solid State* **23** 1022 (1981)]
17. Ando T, Wakahara S, Akera H *Phys. Rev. B* **40** 11609 (1989)
18. Einevoll G T, Sham L J *Phys. Rev. B* **49** 10533 (1994)
19. Morrow R A, Brownstein K R *Phys. Rev. B* **30** 678 (1984)
20. Vas'ko F T *Pis'ma Zh. Eksp. Teor. Fiz.* **30** 574 (1979) [*JETP Lett.* **30** 541 (1979)]
21. Zhu Q G, Kroemer H *Phys. Rev. B* **27** 3519 (1983)
22. Eppenga R, Schuurmans M F H, Colak S *Phys. Rev. B* **36** 1554 (1987)
23. Foreman B A *Phys. Rev. B* **48** 4964 (1993)
24. Ivchenko E L, Kaminski A Yu, Rössler U *Phys. Rev. B* **54** 5852 (1996)

PACS numbers: 04.40.Dg, **95.30.–k**, 97.60.Bw

Explosion mechanisms of supernovae: the magnetorotational model

N V Ardelyan, G S Bisnovatyĭ-Kogan,
S G Moiseenko

1. Introduction

Supernovae appear at the very last stage of evolution of massive stars. The evolution, associated with nuclear burning and generation of more and more massive elements with increasing binding energies, ends up either with a nuclear explosion during the formation of a degenerate carbon-oxygen core of about 1.5 solar masses, or with a loss of stability and collapse of the core consisting of elements from the iron group. The collapse terminates when a stable neutron star forms at the centre. During neutron star formation, a huge quantity of energy is released, nearly 20 percent of the stellar rest-mass energy, but almost all the energy is liberated as the weakly interacting and elusive neutrinos. To explain the supernova explosion which accompanies the formation of a neutron star, less than 0.1% of the neutrino energy would be sufficient, but the use of even so tiny a fraction is not always possible and one meets difficulties in producing the explosion. To date, after 30 years of hard work on this issue, the conclusion is inferred that an explosion is impossible in a simple spherically symmetric model, which was first considered in Ref. [21].

An explosion can be attained in two cases. In the first variant one assumes the development of a convective instability, which increases the energy of escaping neutrinos, and leads to the explosion. This model is sensitive to the initial physical parameters, to the convection treatment, and even to the computational scheme used. The explosion obtained in three-dimensional calculations does not provide a final assurance because of the inevitable increase of numerical errors [12, 13, 15, 20].

The second model utilizes a conversion of the rotational energy of a neutron star with a mantle into the energy of expanding matter, with the use of the magnetic field as the transferring agent. In these calculations, the energy conversion coefficient of a few percent is steadily obtained in different approximations. This proves to be enough to explain a supernova explosion. Firstly, the field is amplified by differential rotation, and then such a magnified field leads to the conversion of the rotational energy into the energy of explosion. After that the magnetic field returns to its initial strength, and the star becomes rigidly and comparatively slowly rotating.

2. Basic equations of the magnetorotational model of explosion

The magnetorotational model for a supernova explosion was suggested in paper [7], and one-dimensional calculations were published in Refs [1, 11]. Two-dimensional calculations using an implicit Lagrangian scheme with a triangular grid have been started in papers [2, 3]. In the subsequent papers [4–6], the computations were performed with an improved grid with readjustment. In Refs [5, 6], the magnetorotational explosion of a rotating cloud was first simulated, and calculations of a supernova explosion taking account of a realistic equation of state of the superdense neutron star matter and neutrino cooling are presently being carried out [8]. The magnetorotational model of explosion was explored in paper [19], in which a spherically symmetric model was used in one-dimensional calculations, as well as in papers [17, 23], in which two-dimensional calculations were performed with an Eulerian grid that does not permit the treatment of large jumps of the parameters, using a simplified magnetic-field structure and assuming a highly overstated field strength. The results of these works, in which an effective explosion was obtained, does not allow us, however, to make conclusions about its form, time scale, and other observable characteristics. Notice that the magnetorotational mechanism was considered in paper [16] for the glowing of the Crab nebula to be explained through the winding of its magnetic field by a rotating neutron star.

The system of equations of magnetic gas dynamics describing a magnetorotational supernova explosion has the form

$$
\begin{aligned}
&\frac{\mathrm{d}\mathbf{x}}{\mathrm{d}t} = \mathbf{u}\,, \qquad \frac{\mathrm{d}\rho}{\mathrm{d}t} + \rho \operatorname{div}\mathbf{u} = 0\,,\\
&\rho\,\frac{\mathrm{d}\mathbf{u}}{\mathrm{d}t} = -\operatorname{grad}\left(p + \frac{\mathbf{B}\cdot\mathbf{B}}{8\pi}\right) + \frac{1}{4\pi}\operatorname{div}(\mathbf{B}\otimes\mathbf{B}) - \rho\operatorname{grad}\Phi\,,\\
&\rho\,\frac{\mathrm{d}}{\mathrm{d}t}\left(\frac{\mathbf{B}}{\rho}\right) = \mathbf{B}\cdot\nabla\mathbf{u}\,,\\
&\rho\,\frac{\mathrm{d}\varepsilon}{\mathrm{d}t} + p\operatorname{div}\mathbf{u} = 0\,, \qquad \eta = \frac{1}{\rho} = \frac{TR}{p}\,, \qquad \varepsilon = \frac{TR}{\gamma - 1}\,,\\
&\Delta\Phi = 4\pi G\rho\,. \qquad (1)
\end{aligned}
$$

The problem is considered in a cylindrical frame of reference under the assumption of equatorial (symmetry plane $z = 0$) and axial ($\partial/\partial\varphi = 0$) symmetry. Here $\mathrm{d}/\mathrm{d}t = \partial/\partial t + \mathbf{u}\cdot\nabla$, $\mathbf{x} = (r, \varphi, z)$ is the radius-vector of a continuous medium particle in cylindrical coordinates, $\mathbf{u}$ is the velocity vector, ρ is the density, p is the pressure, $\mathbf{B}$ is the magnetic field strength, Φ is the gravitational potential, ε is the internal energy, G is the Newtonian constant of gravitation, R is the molar gas constant, and γ is the adiabatic index. The problem is being solved in a bounded region beyond which the density vanishes. The poloidal components of the magnetic field B_r, B_z can be nonzero outside the cloud as well.

3. Results of one-dimensional calculations

In a one-dimensional setting of the problem, an axially homogeneous cylinder with $v_z = B_z = j_r = j_\varphi = 0$ is considered. This corresponds to neglecting motions along the axis z in a real star. The one-dimensional nonstationary MHD equations were solved inside the region $R_0 < r < R(t)$, where R_0 is the radius of a rigidly rotating core with a mass M_0 per unit length. Under cylindrical symmetry the condition of conservation of the magnetic flux radial component reduces to the equality $rB_r = A = \text{const}$. Let the mass per unit length of the mantle be M. The problem has two dimensionless parameters

$$
\alpha = \frac{A^2}{4\pi M V_0^2} \qquad (V_0 = \sqrt{2\pi G M_0}\,)\,, \qquad \beta = \frac{M_0}{M}\,. \qquad (2)
$$

Calculations [1] were carried out for $\beta = 1$, $\alpha = 10^{-2}$, 10^{-4}, 10^{-8}. They demonstrated that the solution tends to a universal one at small α, when the characteristic time scales of processes increase as $\sim \alpha^{-1/2}$, and functions $v_{r\alpha} = v_r\alpha^{-1/2}$,

$h_\alpha = rB_\varphi \alpha^{1/2}$ behave similarly depending on the radius r and the reduced time $t_\alpha = t\alpha^{1/2}$. Figures 1–3 display calculated changes in the distributions of angular velocity and temperature across the mantle, as well as the form of the magnetic force lines at the instant close to that of maximum winding of the force lines. In Fig. 2 one can see the formation and expansion of a shock wave in the mantle, and Fig. 1 shows how the angular velocity of the core decreases during the magnetorotational explosion due to removal of angular momentum by the expelled matter. Under the condition of conservation of the total angular momentum of the core and the mantle, a reversal rotation of the core and adjacent mantle, as well as magnetorotational oscillations arising only in the cylindrical model, become possible. Taking account of the spherical gravitational potential of a real neutron star, one can estimate the mass and kinetic energy of the ejected matter at small α:

$$M_{\rm sh} \approx 0.13 M_\odot\,, \qquad \epsilon_{\rm sh} \approx 0.035 \epsilon_{\rm rot}\,, \tag{3}$$

where $\epsilon_{\rm rot}$ is the total rotational energy of the core-mantle system at the beginning.

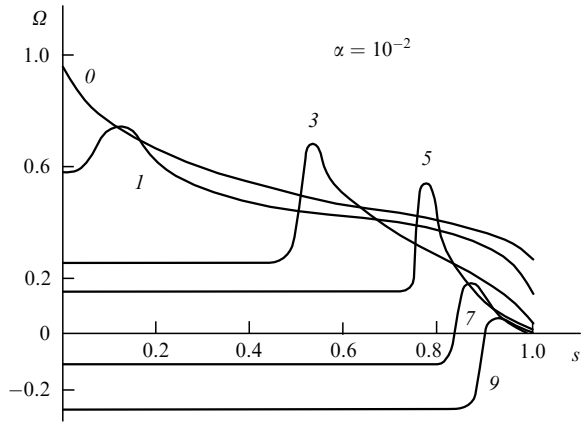

Figure 1. Distribution of angular velocity (normalized to the maximum) over the dimensionless mantle mass.

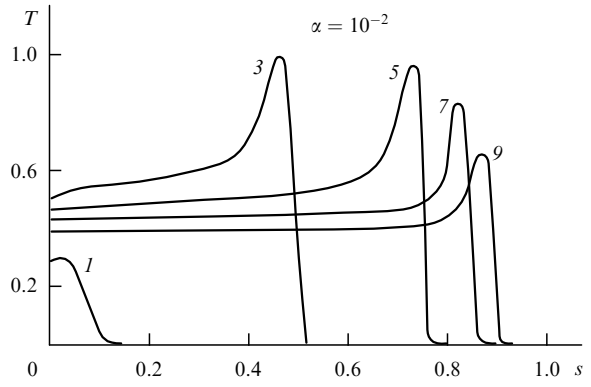

Figure 2. Distribution of temperature (normalized to the maximum) over the dimensionless mantle mass.

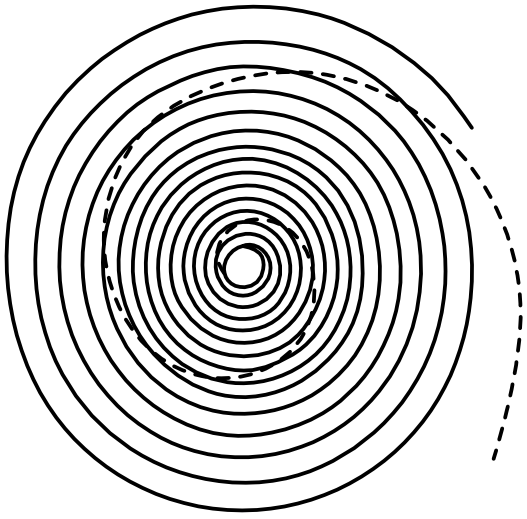

Figure 3. Form of the magnetic force lines in the region near the core at the moment of time close to the maximum winding.

4. 2D calculations in an axially symmetric model

First we consider a rigidly rotating homogeneous gaseous sphere, in which [6]

$$r = 3.81 \times 10^{16}\ {\rm cm}\,, \qquad \rho = 1.492 \times 10^{-17}\ {\rm g\ cm^{-3}}\,,$$
$$M = 1.73 M_\odot = 3.457 \times 10^{33}\ {\rm g}\,,$$
$$\gamma = \frac{5}{3}\,, \qquad u_r = u_z = 0\,,$$
$$\frac{E_{\rm rot0}}{E_{\rm gr0}} = 0.04\,, \qquad \frac{E_{\rm in0}}{E_{\rm gr0}} = 0.01\,. \tag{4}$$

The cloud starts collapsing and after several oscillations arrives at a quasi-stationary state. At this stage the rotation of the cloud becomes differential. The stationary central density is $\rho_{\rm c} \approx 400\rho_0$. By the moment $t_1 = 5.15$ (in dimensionless units related to the characteristic collapse time), a magnetic field with a configuration close to a quadrupole 'turns on'. The ratio of the magnetic field energy at the 'turn-on' moment to the gravitational energy of the cloud at this moment is $E_{\rm magl}/E_{\rm grl} = 0.05$. A toroidal magnetic field component appears owing to the differential rotation of the cloud, which grows with time and leads to a magnetic pressure increase inside the cloud. The maximum of the toroidal magnetic field component is in the equatorial plane of the cloud and moves toward the cloud centre with time. By the time $t = 10.2$, the toroidal magnetic field energy reaches its maximum. After that the toroidal magnetic energy decreases with time.

Beginning from the moment of the magnetic field turn-on at $t = 5.15$ until the moment $t = 10.2$, when the toroidal part of the magnetic field energy reaches its maximum, the velocities in the cloud are small. Starting from $t = 10.2$, the cloud expands under the action of the magnetic pressure, mostly in the equatorial plane. Beginning from $t = 11.3$, the outer parts start acquiring sufficient kinetic energy to escape to infinity. Equatorial matter outflow changes the form of the cloud, which is shown in Fig. 4 for the last moment of the calculations at $t = 32.6$. Figure 5 demonstrates the increase of mass of the ejected matter, whose kinetic energy reaches almost one percent of the gravitational energy of the ultimate cloud configuration.

The results obtained show the high efficiency of the magnetorotational explosion mechanism, reaching one percent of the gravitational energy in the case of a cloud. For a supernova explosion with the formation of a neutron star, an

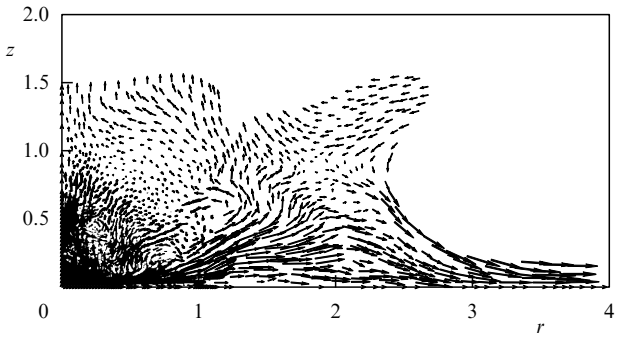

Figure 4. Velocity field in the meridian cut of the cloud at the time $t = 32.6$.

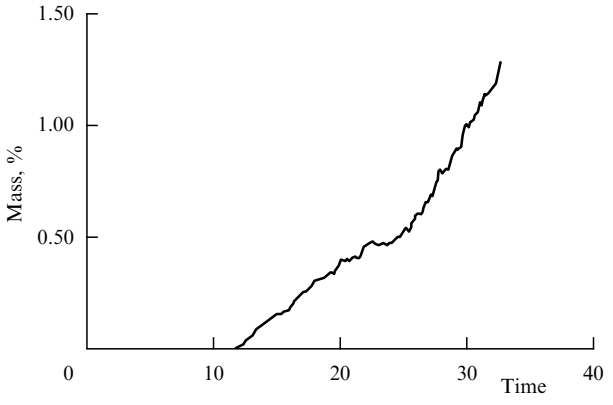

Figure 5. Ejected mass growth as a function of time.

efficiency of about 0.25 percent of the binding energy would be enough, which is near 3 percent of the energy of rotation of a newborn neutron star with the maximum possible angular velocity.

5. Violation of magnetic-field mirror symmetry and the formation of rapidly moving pulsars

Radiopulsar timing research and measurement of their proper motions have revealed that many pulsars move with very high velocities, sometimes exceeding 1000 km s^{-1} [18]. Since pulsars originate from massive stars residing in the galactic disc, whose peculiar velocity is much lower, they most probably acquired such high velocities during neutron star formation in consequence of supernova collapse and explosion. In the magnetorotational model, a natural mechanism for the acceleration of a neutron star appears during the collapse. It is based on the violation of the mirror symmetry of the magnetic field in differentially rotating stars, which have different symmetries of the initial poloidal and toroidal fields [9]. As an example one can consider a combination of a dipole and a symmetric toroidal fields, or a quadrupole and antisymmetric toroidal fields in a rigidly rotating pre-supernova. Consider the case with a dipole field. A differential rotation inevitably emerges as a result of the stellar collapse, and the winding of the radial component of the dipole field would lead to the formation of an *antisymmetric* component of the toroidal field, which, added to the initial *symmetric* component, would violate the mirror symmetry of the magnetic field.

The dipole components of the magnetic field in radiopulsars reach 10^{13} G and their toroidal components may be even higher by a few orders of magnitude, like the field in solar spots, which is apparently connected with the toroidal component of the solar magnetic field. Even higher temporary fields are feasible at the stage of the magnetorotational explosion. For such strong fields exceeding the characteristic magnetic field, $B_c = m_e^2 c^3/e\hbar = 4.4 \times 10^{13}$ G (when the energy corresponding to the difference between Landau levels matches $m_e c^2$), the dependence of the weak interaction cross-section on the magnetic field becomes significant due to the change of the phase space volume and the wave function of electrons. For very strong fields, the beta-decay cross-section increases linearly with the field [22]. If the energy of a beta-transition is $\varepsilon_\beta = \Delta m_e c^2$, then the magnetic field effect becomes significant at $B > \Delta B_c$, which for $\Delta = 10-20$ would require fields with $B > 5 \times 10^{14}$ G, which could be appreciably augmented during the magnetorotational explosion. The difference in the weak interaction cross-sections in two hemispheres of the neutron star would lead to a difference in neutrino energy flux, inversely proportional to the interaction cross-section for the neutrino heat transfer [14].

Using the neutrino cooling curve [21] and assuming a linear law for the induced toroidal field growth, which results in the total toroidal field in two hemispheres changing by the law

$$B_\pm \equiv B_{\varphi\pm} = a \pm bt\,, \qquad a = B_{\varphi 0}\,, \qquad b = \frac{|B_p|}{P}\,, \tag{5}$$

we calculated the recoil velocity of the neutron star due to the anisotropic neutrino flux [10]:

$$v_{nf} = \frac{2}{\pi}\,\frac{c}{10}\,\frac{P}{20\text{ s}}\,x\left[0.5 + \ln\left(\frac{20\text{ s}}{P}\,\frac{1}{x}\right)\right]$$
$$\approx x\left(0.5 + \ln\frac{2\times 10^4}{x}\right) \times 1\text{ km s}^{-1}\,. \tag{6}$$

Here the rotation period of the newborn neutron star is $P = 10^{-3}$ seconds, the neutrino pulse duration is 20 seconds with luminosity $L_\nu = 0.1 M_n c^2/20$ s, c is the speed of light, and x is the ratio between the initial toroidal and poloidal fields. For $x = B_{\varphi 0}/|B_p|$ from 20 to 10^3 we get v_{nf} from 140 to 3000 km s^{-1}. As follows from (6), the neutron star velocity acquired by this mechanism has a maximum, as a function of x, which with the same poloidal field gives the characteristic function with a maximum and a decrease for weak and strong fields for the dependence of the radiopulsar velocity on the dipole magnetic field. Unfortunately, observations have not so far allowed us to confirm or refute this dependence because of the significant influence of selection effects.

This work was financially supported by the Russian Foundation for Basic Research (grants Nos 96-02-16553 and 96-01-00838), INTAS (grant No. 93-93), NSF (grant AST-932-0068), and CRDF (grant Rp1-173).

References

1. Ardelyan N V, Bisnovatyĭ-Kogan G S, Popov Yu P *Astron. Zh.* **56** 1244 (1979) [*Sov. Astron.* **23** 705 (1979)]
2. Ardelyan N V et al. *Astron. Zh.* **64** 495 (1987) [*Sov. Astron.* **31** 261 (1987)]
3. Ardelyan N V et al. *Astron. Zh.* **64** 761 (1987) [*Sov. Astron.* **31** 398 (1987)]
4. Ardeljan N V et al. *Astron. Astrophys. Suppl.* **115** 573 (1996)

5. Ardeljan N V, Bisnovatyi-Kogan G S, Moiseenko S G *Astrophys. Space Sci.* **239** 1 (1966)
6. Ardeljan N V, Bisnovatyi-Kogan G S, Moiseenko S G, in *Proc. Int. Workshop* "*SN1987A: Ten Years After*" held in La Serena, Chile on February 22–28, 1997
7. Bisnovatyĭ-Kogan G S *Astron. Zh.* **47** 813 (1970)
8. Bisnovatyĭ-Kogan G S *Fizicheskie Voprosy Teorii Zvezdnoĭ Évolyutsii* (Physical Problems of the Star Evolution Theory) (Moscow: Nauka, 1989)
9. Bisnovatyĭ-Kogan G S, Moiseenko S G *Astron. Zh.* **69** 563 (1992)
10. Bisnovatyi-Kogan G S *Astron. Astrophys. Trans.* **3** 287 (1993)
11. Bisnovatyi-Kogan G S, Popov Yu P, Samochin A A *Astrophys. Space Sci.* **41** 287 (1976)
12. Burrows A, Hayes J, Fryxell B A *Astrophys. J.* **450** 830 (1995)
13. Herant M et al. *Astrophys. J.* **435** 339 (1994)
14. Imshennik V S, Nadezhin D K *Zh. Eksp. Teor. Fiz.* **63** 1548 (1972) [*Sov. Phys. JETP* **36** 821 (1973)]
15. Janka H-T, Muller E *Astrophys. J. Lett.* **448** L109 (1995)
16. Kardashev N S *Astron. Zh.* **41** 807 (1964)
17. Le Blank L M, Wilson J R *Astrophys. J.* **161** 541 (1970)
18. Lyne A G, Lorimer D R *Nature* (London) **369** 127 (1994)
19. Muller E, Hillebrandt W *Astron. Astrophys.* **80** 147 (1979)
20. Miller D S, Wilson J R, Mayle R W *Astrophys. J.* **415** 278 (1993)
21. Nadyozhin D K *Astrophys. Space Sci.* **53** 131 (1978)
22. O'Connell R F, Matese J J *Nature* (London) **222** 649 (1969)
23. Ohnishi T *Tech. Rep. Inst. At. Energy Kyoto Univ.* (198) 1 (1983)

PACS numbers: **95.30.–k**

Stars, planets, and cosmic masers

V I Slysh

As early as 1966, immediately after OH masers have been discovered, I S Shklovskiĭ proposed to connect cosmic masers with star formation processes. The formation of a star can be also accompanied by the formation of its planetary system from the surrounding gas-dust protoplanetary disk which appears as an angular momentum reservoir. The protostar may shrink and accrete fresh matter only providing its own angular momentum is transferred to the disk. Consequently, disks around stars exhibit the generic attribute of protostars. The disk can in turn fragmentate into ring zones with the subsequent formation of planets. Such a picture, suggested in general form by Kant and Laplace, is presently being confirmed due to emerging of new observational methods with a high angular resolution. Planets are discovered around 20 near stars of the main sequence, with the mass of 9 planets being less than 13 Jupiter masses, the latter is known to be a conventional border between planets and low-mass stars called brown dwarfs. High resolution of the Hubble Space Telescope allowed astronomers to find numerous evidences of star formation processes under way and to obtain images of very dense blobs of matter — globules, as well as individual protostars surrounded by gas-dust disks. They were called 'proplydes', the precursors of planetary systems. The disk near β Pictoris may provide such an example as well.

Radiointerferometric systems, which are used to obtain images of maser sources, have an even higher angular resolution of 0.1 milliarcsecond corresponding to 0.1 AU linear size at a distance of 1 kpc, which is much smaller than the typical planetary system size. Since masers turned out to be closely connected to star formation regions and are bright enough for radiointerferometric studies, they may be used for searching and exploring protoplanetary systems at different evolutionary stages. Recently, in addition to well-known OH and H_2O masers, new methanol masers were discovered which are sensitive indicators of physical conditions. Studies of masers have established that they are related to several different stages in the evolution of protostars and planetary systems. Methanol masers of class II and OH masers emerge in peripherical remnants of the disks around young hot stars with a high mass ($50M_\odot$) at a distance of several thousand astronomical units from the star. These masers are probably correlated with extended atmospheres of ice planets (giant comets). Some H_2O masers (such as IC1396N) are associated with disks around protostars of low mass ($0.1M_\odot$) which are still accreting matter. These disks are not large in size, of order 20 AU. Even more earlier stage of protostar evolution, cold dense nuclei in molecular clouds, is connected with methanol masers of class I (OMC-2, NGC2264).

Similar phenomena, disks with maser sources, were discovered in much larger scales in nuclei of some active galaxies around black holes with masses of $10^6-10^9M_\odot$.